

1

1 The effect of elevated carbon dioxide on the sinking and swimming of the shelled pteropod

2 *Limacina retroversa*

3

4 Alexander J. Bergan¹, Gareth L. Lawson^{1*}, Amy E. Maas^{1,2}, Zhaohui Aleck Wang³

5

6 1. Biology Department, Woods Hole Oceanographic Institution, Woods Hole, MA,

7 USA

8 2. Bermuda Institute of Ocean Sciences, St. George's GE01, Bermuda

9 3. Marine Chemistry and Geochemistry Department, Woods Hole Oceanographic

10 Institution, Woods Hole, MA, USA

11

12 *Corresponding author: tel: +508 289 3713; e-mail: glawson@whoi.edu

13

14 *Keywords: ocean acidification, shell condition, locomotion, thecosome pteropod*

15

16 **Abstract**

17 Shelled pteropods are planktonic molluscs that may be affected by ocean
18 acidification. *Limacina retroversa* from the Gulf of Maine were used to investigate the
19 impact of elevated carbon dioxide (CO₂) on shell condition as well as swimming and
20 sinking behaviours. *Limacina retroversa* were maintained at either ambient (ca. 400 µatm)
21 or two levels of elevated CO₂ (800 and 1200 µatm) for up to four weeks, and then
22 examined for changes in shell transparency, sinking speed, and swimming behaviour
23 assessed through a variety of metrics (e.g., speed, path tortuosity, wing beat frequency).
24 After exposures to elevated CO₂ for as little as four days, the pteropod shells were
25 significantly darker and more opaque in the elevated CO₂ treatments. Sinking speeds were
26 significantly slower for pteropods exposed to medium and high CO₂ in comparison to the
27 ambient treatment. Swimming behaviour showed less clear patterns of response to
28 treatment and duration of exposure, but overall, swimming did not appear to be hindered
29 under elevated CO₂. Sinking is used by *L. retroversa* for predator evasion, and altered
30 speeds and increased visibility could increase the susceptibility of pteropods to predation.

31

32 **Introduction**

33 The chemistry of the oceans is rapidly changing due to the infiltration of
34 anthropogenic carbon dioxide (CO₂) into the surface ocean, a process known as ocean
35 acidification. One of the effects of ocean acidification is a decrease in the availability of
36 carbonate ion (CO₃²⁻) which affects calcifying organisms that use calcium carbonate
37 (CaCO₃) to build shells and other structures (e.g. Orr *et al.* 2005, Royal Society 2005). A
38 shifting balance of dissolution and calcification as saturation state decreases due to ocean

39 acidification jeopardises the shell structure that, in many cases, provides protection from
40 predators (e.g. Fabry *et al.* 2008). Ocean acidification could also change the way that some
41 organisms move in their environment since calcified structures govern the movements of
42 certain planktonic organisms, including echinoderms and molluscs (e.g. Chan *et al.* 2011,
43 Wheeler *et al.* 2013).

44 Thecosomes, or shelled pteropods (Order Euthecosomata; henceforth referred to
45 simply as pteropods), are planktonic molluscs that build calcium carbonate shells in the
46 crystal form of aragonite, which is less stable than the other common form, calcite.
47 Pteropod shells are becoming increasingly soluble in some regions of their habitat due to
48 ocean acidification (e.g. Fabry *et al.* 2008). The shells of many species of pteropod are
49 transparent, but turn darker and more opaque when exposed to seawater under-saturated
50 with respect to aragonite, possibly due to an increased roughness of the shell's surface
51 associated with partial dissolution (Almogi-Labin *et al.* 1986, Haddad and Droxler 1996,
52 Lischka *et al.* 2011, Lischka and Riebesell 2012, Wall-Palmer *et al.* 2013). Laboratory
53 experiments have also shown that lowering the saturation state decreased calcification,
54 leading to impaired shell growth (Comeau *et al.* 2009, Comeau *et al.* 2010, Bednaršek *et*
55 *al.* 2014). Wild caught *Limacina helicina* from regions naturally low in aragonite
56 saturation state have also shown signs of dissolution under scanning electron microscopy
57 (Bednaršek, *et al.* 2012, Bednaršek, *et al.* 2014, Bednaršek, and Ohman. 2015).

58 Shelled pteropods are a food source for many marine organisms, including
59 seabirds, whales, salmon, trout, mackerel, cod, myctophids, and other zooplankton
60 (LeBrasseur 1966, Ackman *et al.* 1972, Conover and Lalli 1974, Levasseur *et al.* 1996,
61 Pakhomov *et al.* 1996, Armstrong *et al.* 2005, Hunt *et al.* 2008, Karnovsky *et al.* 2008,

62 Pomerleau *et al.* 2012, Sturdevant *et al.* 2013), and hence any effects of ocean acidification
63 on pteropod populations also could have effects on a wide range of marine species. The
64 ability of pteropods to move through the water column could be affected by ocean
65 acidification via changes to the shell. Pteropods have evolved wings, or parapodia, to
66 propel themselves through the water. The spiral shaped pteropod species (Limacinidae)
67 swim in a zig-zag motion, rotating their shell between a power stroke followed by a
68 recovery stroke to provide lift (Chang and Yen 2012, Murphy *et al.* 2016). Many species
69 of pteropods make daily migrations to depth during the day to avoid visual predators and to
70 the surface at night to feed (Wormuth 1981, Comeau *et al.* 2012, Maas *et al.* 2012);
71 sinking of the negatively buoyant shell is presumed to be an important component of the
72 downward part of this diel vertical migration. Pteropods can also use swimming and
73 sinking to escape from predators that are in their immediate proximity (Comeau *et al.*
74 2012). Harbison and Gilmer (1986) observed both swimming and sinking behaviours when
75 pteropods were disturbed. Furthermore, after pteropods die, their sinking shells sequester
76 inorganic carbon to the deep ocean (Byrne *et al.* 1984) and pteropod shells are estimated to
77 account for 12% of the global carbonate flux (Berner and Honjo 1981). Changes in the
78 fitness, abundance, and sinking of pteropods under ocean acidification thus also have
79 consequences to the carbon cycle.

80 The species examined in this study, *Limacina retroversa*, is found in the Gulf of
81 Maine, a region that is particularly susceptible to ocean acidification (Wang *et al.* 2013).
82 Due to deep water formation in the North Atlantic, the infiltration of anthropogenic CO₂
83 into intermediate and deep water is pronounced in this region and is causing the carbonate
84 chemistry throughout the water column to change more quickly than the average global

85 rate (Sabine *et al.* 2004). Furthermore, recent studies along the length of the U.S. East
86 Coast found that the Gulf of Maine had the lowest saturation states observed as well as the
87 lowest total alkalinity to dissolved inorganic carbon ratio, indicative of strong sensitivity to
88 continued acidification (Wang *et al.* 2013; Wanninkhof *et al.* 2015). Although found year
89 round in the Gulf of Maine, *L. retroversa* is also found in the open ocean, in the temperate
90 and subpolar Atlantic of the Northern and Southern hemispheres. As a broadly distributed
91 species that is also readily available relatively close to shore, it serves as a useful model
92 species for examining the response of pteropods to ocean acidification.

93 In this study, *L. retroversa* were captured and reared under different concentrations
94 of CO₂ over the course of multiple seasons to examine the impacts on shell condition and
95 locomotion, testing the hypotheses that 1) The appearance of shells changes after exposure
96 to elevated levels of CO₂; 2) *L. retroversa* sinking speed differs among CO₂ treatments;
97 and 3) The swimming ability of *L. retroversa* is affected by exposure to elevated CO₂.

98

99 **Methods**

100 Four cruises into the Gulf of Maine allowed for the capture of shelled pteropods,
101 *Limacina retroversa*. The pteropods were brought back to the laboratory and reared in
102 seawater modified by bubbling with three different levels of CO₂, an ambient treatment
103 (nominally 400 ppm) and two elevated treatments, 800 and 1200 ppm, hereafter referred to
104 as the ambient, medium, and high CO₂ treatments, respectively. These were intended to
105 yield over-saturated, marginal, and strongly under-saturated conditions with respect to
106 aragonite. The actual pCO₂ levels and saturation states achieved via bubbling were
107 calculated from measured dissolved inorganic carbon (DIC) and total alkalinity (TA) using

108 CO2SYS (see below). The condition of shells along with swimming performance and
109 sinking rates of animals was examined after 2 days to 4 weeks of exposure.

110

111 *Animal Sampling*

112 *Limacina retroversa* were collected in water depths of ca. 45-260 m in the Gulf of
113 Maine near Provincetown, MA aboard the R/V *Tioga* during four cruises in April, August,
114 and November 2014 and April 2015, with each expedition lasting one to three days.

115 Oblique tows were conducted with a 1-m diameter Reeve net with 333 μm mesh size. The
116 net was equipped with a large cod-end and hauled at slow speeds (ca. 5 m/min) to collect
117 animals in healthy condition. *Limacina retroversa* were isolated from the rest of the
118 plankton sample and placed into 1-L jars filled with Gulf of Maine seawater pumped *in*
119 *situ* from a depth of ca. 30 m and filtered through a 64 μm sieve. The pteropods were kept
120 at densities of ca. 30-40 individuals per litre and maintained in a refrigerator at ca. 8°C and
121 later in coolers for transfer to the laboratory.

122

123 *Culturing and Experimental Set-up*

124 Upon returning to the laboratory, *L. retroversa* were moved with a soft pipette into
125 13-L carboys with 2-3 replicate carboys per treatment. The carboys were filled with *in situ*
126 seawater collected during the cruise that had been transferred a day earlier to the laboratory
127 and filtered to 1 μm . For the duration of each experiment, as well as for ca. 8-16 hours prior
128 to the addition of animals, each carboy was bubbled continuously using one of the three
129 CO₂ concentrations, ambient (nominally ca. 400 ppm), 800, and 1200 ppm. For the
130 medium and high treatments, the target air-balanced CO₂ gases used for bubbling were

131 achieved by mixing pure CO₂ gas and CO₂-free air using mass-flow controllers. The
132 ambient treatment was not controlled but rather was derived from the CO₂ content of
133 ambient air drawn from outside the building.

134 The carboys were kept in a cold room at 8°C at a density of ca. 15 individuals per
135 litre. The pteropods were fed a mixed diet of *Rhodomonas lens* (1500-4000 cells/mL) and
136 *Heterocapsa triquetra* (150-500 cells/mL) with lower concentrations provided over the
137 course of each experiment as the pteropod culture density decreased due to mortality and
138 use for various measurements. Water and pteropods were siphoned out of the carboys
139 every week so that the seawater could be replaced with clean pre-bubbled water (collected
140 *in situ* in the Gulf of Maine and kept after the cruise in a holding tank filtered continuously
141 at 1 µm) and dead pteropods could be separated from the live ones. Additional details on
142 culturing protocols can be found in Thabet *et al.* (2015).

143 During water changes, samples of the water leaving each carboy and the water
144 entering the carboys were collected in 250 mL borosilicate glass bottles, poisoned with 100
145 µL saturated mercuric chloride, and then capped with a greased stopper for later analysis of
146 TA and DIC. TA was measured using an Apollo SciTech alkalinity auto-titrator (AS-
147 ALK2, Apollo SciTech, Newark, DE, USA), an Orion 3 Star pH metre, and a Ross
148 combination pH electrode based on a modified Gran titration method (Wang and Cai
149 2004). DIC was analysed with a DIC auto-analyzer (AS-C3, Apollo SciTech, Newark, DE,
150 USA) via acidification and non-dispersive infrared CO₂ detection (LiCOR 7000: Wang and
151 Cai 2004). The saturation state of aragonite (Ω_A), pCO₂, and pH were calculated from DIC
152 and TA with the CO2SYS software (Pierrot *et al.* 2006), using constants K₁ and K₂ from

153 Mehrbach *et al.* (1973) refitted by Dickson and Millero (1987), and the KHSO_4
154 dissociation constant from Dickson (1990).

155 In order to monitor conditions and adjust bubbling rates accordingly between water
156 changes, pH in each carboy was measured every 2-3 days using a USB 4000 spectrometer
157 with an LS-1 light source and a FIA-Z-SMA-PEEK 100-mm flow cell (Ocean Optics,
158 Dunedin, FL, USA), and 2 mM m-Cresol indicator dye (50 μL in 20 mL of sample). The
159 DIC/TA-based calculations of Ω_A and pCO_2 described above were used as the primary
160 means of assessing the carbonate chemistry of the experimental treatments, but Ω_A and
161 pCO_2 were also calculated using CO2SYS from measurements of pH along with the
162 nearest measurement of TA in time, as a means of assessing variability between water
163 changes.

164

165 *Shell Condition*

166 Ten live animals were removed from each of the ambient, medium, and high
167 treatments at days 2, 4, 8, and 15 during the April 2015 experiment. They were rinsed in
168 deionised water, weighed wet and dry with a Cahn C-33 microbalance with a precision of
169 1 μg , then placed in 8.25% hypochlorite bleach for 24-48 hours to remove tissue, rinsed in
170 deionised water again, and dried.

171 Using a light microscope, the empty shells were photographed at 2.5X
172 magnification for transparency, opacity, and length measurements. For transparency, the
173 shell was positioned in a glass petri dish with the aperture facing up and the light coming
174 from below and through the shell. A photograph was taken through the microscope with a
175 2-ms exposure, and with white balance, contrast, and brightness values conserved across

176 images. Similarly, opacity was measured from images of shells placed with the aperture up
177 with 2-ms exposure, but with the lighting coming from two iridescent lights that
178 illuminated the shell parallel to the camera in order to measure reflected light. The lights
179 were positioned opposite each other to reduce shadows, and about 10 cm away from the
180 shell's location at the centre of the petri dish.

181 Images were analysed in MATLAB to calculate transmittance and opacity. For
182 transmittance, the shell was identified against the white background by thresholding the
183 image to black and white. The aperture as well as any holes were manually cropped from
184 the object. The transmittance was calculated as the mean grayscale value (range: 0-255) of
185 the pixels of the shell divided by 255 to get a scale of 0 (black) to 1 (white). The image
186 analysis was similar for opacity, but instead the shell was identified by thresholding the
187 brighter shell from a dark background. For opacity the mean grayscale value of the shell,
188 after cropping out the aperture and any holes, was calculated on the same scale of 0 (black)
189 to 1 (white), like transmittance.

190

191 *Videography*

192 Live and active *L. retroversa* (shell lengths ranging from 0.56 mm to 2.37 mm)
193 were removed from each of the CO₂ treated carboys for filming during the 1st, 2nd, 3rd, and
194 4th weeks of exposure to the different CO₂ treatments. Due to the length of time needed to
195 make a sufficient number of observations, filming was done over two to five days for each
196 week. The exact numbers removed from the treatments for each week as well as which
197 weeks were sampled varied among experiments due to variability in the number of live
198 animals available and needs for companion studies of physiology and gene expression. The

199 removed animals were moved to another cold room at 8°C, in 1-L jars of filtered seawater
200 at the ambient CO₂ concentration. Videos were recorded with a Photron Fastcam SA3 high
201 speed camera at 500 frames per second. A triangular prism tank with a mirrored face on
202 the hypotenuse of the isosceles right triangle was used so that both the animal and its
203 orthogonal projection were visible in the field of view and the 3D position and velocity of
204 the pteropod could be recorded (Figure 1a). Illumination was delivered by an LED panel
205 with the light diffusing through a thin plastic sheet. The mirrored tank was filled with
206 filtered seawater with a density between 1024-1026 kg/m³. Density was measured with a
207 digital seawater refractometer (Hanna Instruments, model 96822). Three types of
208 movements were examined: sinking with wings withdrawn, sinking with wings extended,
209 and upward swimming.

210

211 *Sinking*

212 For quantification of sinking rates, a rigid pipette was attached to a ring stand and
213 placed so that the narrow end was in the water and at the top of the camera's frame (Figure
214 1b,c). The camera was focused and a ruler used to calibrate distance in the tank. The field
215 of view for sinking trials was 5.7 cm x 5.7 cm. Each *L. retroversa* was sucked into a soft
216 pipette and then released into the fixed pipette. The constriction in the fixed pipette caused
217 the animal to slow and then accelerate as it left the fixed pipette and sank through the
218 frame. Individual animals were filmed for 3-6 repeat sinking trials, which were used to
219 calculate average sinking rates for each experimental animal later used in statistical
220 comparisons among treatments. In April, August, and November of 2014, animals were
221 filmed sinking with their wings extended and also with their wings withdrawn. In April

222 2015, only animals sinking with wings withdrawn were recorded in order to dedicate more
223 time and generate a larger sample sizes for this behaviour, since by then the difference
224 between wings withdrawn and wings extended during sinking had already been
225 determined.

226 The videos were analysed in MATLAB by converting the frames to black and
227 white. With the pteropod and its reflection isolated as objects, the length and position of
228 the animal and its reflection were measured. Over successive frames, the difference in
229 position was used to calculate speed. Since the animals rotated slightly about the horizontal
230 axis the maximum length of the animal or reflection observed over the course of the video
231 was used to estimate the length of the long axis. Speed vs. time plots were fit with a
232 hyperbolic tangent function, giving an analytical solution for terminal speed. The
233 hyperbolic tangent function solves for sinking velocity for a high Reynolds number regime
234 (Owen and Ryu 2005). The Reynolds number is a non-dimensional number describing the
235 ratio of inertial to viscous forces and is calculated here as animal length multiplied by the
236 speed of the pteropod divided by the kinematic viscosity of water. Although *L. retroversa*
237 move at low to intermediate Reynolds numbers (ca. 5-50), the hyperbolic tangent function
238 fit the data better than the low Reynolds number solution (negative exponential function).

239

240 *Swimming*

241 Swimming trials were conducted by placing animals below the camera's field of
242 view via soft pipette and filming their swimming up through the frame. The size of the
243 field of view was calibrated with a ruler and was 2.7 cm x 2.7 cm, with the bottom of the
244 field of view 2-3 cm above the floor of the tank. In the April 2014 and August 2014

245 experiments, multiple pteropods from the same treatment were placed in the tank together
246 and swimming trials were recorded. Each of these swimming trials was included separately
247 in statistical comparisons among treatments, but since the exact identity of swimmers was
248 not known, the more active individuals could have contributed multiple swimming
249 observations. Therefore, for improved accuracy, in November 2014 and April 2015, a
250 single individual was placed in the tank and multiple swimming trials were recorded for
251 each animal; swimming metrics averaged over the multiple trials for each individual were
252 then used in statistical comparisons among treatments.

253 Video analysis was done in MATLAB with similar protocols as for sinking. The
254 frames were converted to black and white to allow for the identification of the pteropod
255 and its reflection to track its properties (length, position) from one frame to the next. These
256 properties were used to determine the speed, distance travelled, and trajectory. Path
257 tortuosity was measured as the total cumulative distance travelled over a video segment
258 divided by the direct distance between the last and first frame; each video segment was at
259 least 0.5 seconds and recorded at least three wing beats (power and recovery strokes). The
260 swimming metrics examined were the mean speed (calculated in 3D), frequency of wing
261 beats, path tortuosity, ratio of horizontal to vertical displacement, and asymmetry of speed
262 between the power and recovery strokes (Figure 2).

263

264 *Statistics*

265 One-way analyses of variance (ANOVA), or a Kruskal-Wallis one-way ANOVA
266 on ranks when the data failed either the equal variance or normality tests, were used to test
267 for differences among treatments in shell transmittance and opacity, sinking speeds

268 (separately for wings withdrawn and extended), swimming speed, wing beat frequency,
269 swimming path tortuosity, ratio of horizontal to vertical displacement, and asymmetry in
270 speed between the power stroke and recovery stroke. If there were significant effects from
271 these tests, post-hoc pairwise comparison tests were conducted using the Holm-Sidak
272 method for one-way ANOVAs and Dunn's method for Kruskal-Wallis one-way ANOVAs.
273 Sinking speed with wings withdrawn was compared to sinking speed with wings extended
274 using a Wilcoxon Paired-Sample Signed-Rank signed rank test. Correlation coefficients
275 were also calculated among swimming metrics.

276

277 **Results**

278 *Experimental Treatments*

279 The nominal target values for pCO₂ of 400, 800, and 1200 µatm were not always
280 achieved and calculated values varied among experiments, but overall the carbonate
281 chemistry measurements indicated clear distinctions among treatments (summarised in
282 Table 1 and see Supplementary Table S1 for full details). The ambient treatment had
283 higher levels than the nominal 400 µatm (the approximate global average atmospheric
284 concentration), closer to 450 µatm. Calculations of achieved pCO₂ for the medium and
285 high treatments also indicated variability, likely due to a combination of uncertainty in the
286 sampling and measurements of DIC and TA, uncertainty in the mixture of gas by the mass-
287 flow controllers, and variability in the degree of bubbling. In April and August 2014 the
288 calculated pCO₂ of pre-bubbled water that was entering the carboys at the onset of the
289 experiment was consistently lower than that calculated for the outgoing water, suggesting
290 incomplete pre-equilibration (Supplementary Table S1). Subsequent measurements of pH

291 made between water changes, however, indicated that the seawater chemistry for these
292 treatments attained their target values after less than 24 h.

293 Measurements of outgoing water made during water changes indicated that the
294 ambient treatments always had over-saturated conditions with respect to aragonite
295 ($\Omega_A=1.49-1.61$), medium treatments were near the threshold of saturation (0.76 in
296 November 2014, 1.21 in August 2014, and otherwise 0.94-1.05), and the high treatment
297 had strongly under-saturated conditions ($\Omega_A=0.63-0.80$, Table 1). The medium treatment
298 showed the greatest variability, likely due to a combination of sampling error, issues with
299 the mass-flow controllers (in November 2014, where saturation states were overly low),
300 and insufficient bubbling (in August 2014, where saturation states were overly high). The
301 ambient treatment was significantly different in aragonite saturation state from both of the
302 elevated CO₂ treatments in three of the experiments (one-way ANOVA, $p<0.001$), while in
303 the August 2014 experiment only the ambient and high treatments were significantly
304 different (Kruskal-Wallis one-way ANOVA, $H=11.7$, $p=0.003$). The medium and high
305 treatments were also significantly different from one another in April of 2014 and 2015
306 (Holm-Sidak, $p<0.05$), though not in August or November 2014. TA showed relatively
307 small differences between experiments, presumably related to natural seasonal processes in
308 the Gulf of Maine region (Supplemental Table S1).

309

310 *Shell Condition*

311 Shell condition from the April 2015 experiment for the ambient treatment was
312 mostly unchanged relative to duration of exposure, while the medium and high CO₂
313 treatments showed decreased transmittance and increased opacity over the course of 15

314 days of exposure (Figure 3, Table 2). On day 2, there was not a significant difference in the
315 appearance of shells among treatments, but both shell transmittance and opacity were
316 significantly different among treatments on days 4, 8, and 15 (Table 3). Post-hoc pairwise
317 comparisons showed that the transmittance from the ambient and high treatments were
318 significantly different on days 4, 8, and 15 ($p < 0.05$), the medium and high treatments were
319 never significantly different, and the medium and ambient treatments were only
320 significantly different on day 15 ($p < 0.05$). For opacity, on days 4 and 8 only the ambient
321 and high treatments were significantly different ($p < 0.05$), whereas on day 15, each
322 treatment was significantly different from the others ($p < 0.05$).

323 The dry masses of the shells (with animal body tissue present) from April 2015,
324 normalized to length, indicated an overall decrease over the course of the 15 days of
325 exposure and also substantial overlap among treatments (Supplementary Figure S1). Mass
326 normalized to length was significantly different between the CO₂ treatments at days 8
327 (Kruskal Wallis one-way ANOVA, $H=6.1$, $p=0.048$) and 15 (one-way ANOVA, $F=4.1$,
328 $p=0.037$), but not for the earlier time points. At day 8, there were not significant pairwise
329 differences in mass normalized to length among treatments (Dunn's method, $p > 0.05$), and
330 on day 15 only the medium and high treatment were significantly different from one other
331 (Holm-Sidak method, $p < 0.05$).

332

333 *Sinking*

334 Sinking rates showed differences associated with treatment, duration of exposure,
335 experiment, and behaviour (i.e. wings extended or withdrawn). After one week of
336 exposure, sinking rates for animals with wings withdrawn were similar among treatments

337 and showed no significant differences for two of three experiments (Figure 4a, Table 3),
338 while during week one of the third experiment (April 2015) sinking rates differed
339 significantly among treatments. Sinking rates were significantly slower for animals in the
340 elevated CO₂ treatments than in the ambient treatment after two or more weeks of exposure
341 during every experiment. In all pairwise comparisons, the ambient treatment was
342 significantly different from both the medium and high treatments, except for the second
343 week of the November 2014 when only the ambient and high treatments were significantly
344 different ($p < 0.05$).

345 On average there was an 84% reduction in sinking speed for animals holding their
346 wings extended compared to wings withdrawn, and sinking speeds with wings withdrawn
347 and wings extended measured for the same individuals were significantly different
348 (Wilcoxon Paired-Sample Signed Rank, $Z = -8.981$, $p < 0.001$). Sinking rates for animals
349 with wings extended also showed similar trends to those with wings withdrawn with
350 respect to treatment and duration of exposure (Figure 4b). While there were no significant
351 differences among the treatments after one week of exposure, significant differences were
352 observed among treatments after an exposure duration of two weeks and onwards, with
353 significantly faster sinking rates evident for the *L. retroversa* exposed to ambient CO₂
354 compared with the high treatment (November 2014 week 2) or to the medium and high
355 treatments (April 2014 week 4).

356 In order to account for possible uncertainty introduced by any differences in the
357 size of animals among treatments and time points, attempts were also made to normalise
358 the sinking rate measurements relative to individual size. Linear regressions based on log-
359 log plots were used to examine the effect of length on sinking speed of animals with wings

360 withdrawn. The resulting power law scaling relationships between sinking speed and
361 length for the ambient, medium, and high treatments were 0.45, 0.74, and 0.52 respectively
362 (Figure 5), suggesting that normalising the sinking speeds by the square root of length
363 (0.50 scaling) was appropriate. In all but one case, normalising sinking speed by length in
364 this way did not affect the significance of the differences among treatments, with the
365 exception of week one for November 2014. In this case, in contrast to the initial test, when
366 normalised, the Kruskal-Wallis one-way ANOVA showed significant differences among
367 treatments in sinking speeds ($H=7.3$, $p=0.026$) due to faster sinking in the high treatment,
368 followed by the medium, then ambient.

369

370 *Swimming*

371 In contrast to sinking, swimming rates did not differ in a consistent manner among
372 treatments and durations of exposure. For the two experiments (August 2014 and April
373 2015) where observations were made after one week, mean swimming speed was
374 significantly different among treatments but differed in which treatment showed the fastest
375 swimming (Figure 6a, Table 3). Significant differences were not seen among treatments at
376 two or three weeks. There was also not a significant correlation between swimming speed
377 and animal length (Table 4): in the log-log plot of swimming speed vs. animal length the
378 slopes of the linear regressions were nearly zero (see Supplementary Figure S2) and hence
379 no attempts were made to normalise swimming measurements to animal size.

380 For the initial two experiments (April and August 2014) where multiple animals
381 were together in the filming tank and individual swim analyses were not possible, wing
382 beat frequency showed no differences among treatments (Figure 6b, Table 3). For the two

383 later experiments (November 2014 and April 2015), where individual animals were
384 measured separately, a trend of decreasing flapping frequency under elevated CO₂ was
385 evident, and the frequency of wing beats was significantly higher in the ambient treatment
386 compared to the medium and high treatments in week one of the April 2015 experiment,
387 although not in week two of the November 2014 experiment or week two of April 2015.

388 Tortuosity only differed significantly during the initial experiments (April 2014 and
389 August 2014), where multiple animals were placed together during filming (Figure 6c,
390 Table 3). In the November 2014 and April 2015 experiments, no significant differences
391 were seen in tortuosity among the treatments, although there was a high degree of
392 variability during the November 2014 week two experiment, where the ambient treatment
393 had the highest tortuosity due to an outlier (4.05) and low sample size (n=3). The average
394 ratio of horizontal to vertical displacement averaged over all the experiments was
395 0.35 ± 0.15 (\pm standard deviation) and similar to tortuosity there were only significant
396 differences between treatments in April 2014 (Kruskal-Wallis one-way ANOVA, $H=8.7$,
397 $p=0.013$) and August 2014 (Kruskal-Wallis one-way ANOVA, $H=6.9$, $p=0.032$). The
398 asymmetry between the peak speeds of the power and recovery strokes did not differ
399 among treatments for any of the experiments (one-way ANOVA). The average and
400 standard deviation of asymmetry between the power/recovery strokes over all the
401 experiments was $7.2 \pm 5.1\%$ (n=191).

402 There was a significant positive correlation between mean swimming speed and
403 wing beat frequency and a significant negative correlation between wing beat frequency
404 and length (Table 4). The mean swimming speed also had significant negative correlations
405 with both tortuosity and the asymmetry between the speeds of the power and recovery

406 strokes. There were no significant correlations between tortuosity or the asymmetry of the
407 strokes and length.

408

409 **Discussion**

410 The condition of *Limacina retroversa* shells and sinking speeds of live animals
411 were significantly affected by exposure to elevated carbon dioxide. Since the passive
412 motion of sinking was slower in the elevated CO₂ treatments, even for animals with wings
413 withdrawn, this indicates that the slower sinking rates likely relate to differences in the
414 shells. Swimming behaviour showed less clear patterns of variability in relation to
415 treatment and duration of exposure, and overall swimming ability did not appear to be
416 hindered under elevated CO₂.

417

418 *Shell Condition*

419 The appearance of shells changed significantly in the elevated CO₂ treatments.
420 Differences in transmittance and opacity of the shells from the medium and high
421 treatments relative to the ambient treatment were apparent from day four of exposure,
422 while in contrast the shells from the ambient treatment did not change significantly over
423 time. Other studies have found that short exposures to similar CO₂ concentrations (750,
424 880, and 1000 ppm for 7-8 days) can cause changes in shell condition of *L. retroversa*
425 (Lischka and Riebesell 2012, Manno *et al.* 2012) and in the congeneric species *L. helicina*
426 (Lischka *et al.* 2011, Bednaršek *et al.* 2012, Busch *et al.* 2014, Bednaršek *et al.* 2014). The
427 present study adds to these earlier observations by offering a new, quantitative metric for
428 assessing shell condition based on transparency to light-based microscopy and by

429 extending the duration over which effects on shell condition were examined. Although
430 they were measured and considered separately, transmittance and opacity are highly related
431 optical properties and as such expectedly showed very similar patterns (though in opposing
432 directions). Future studies employing our light microscopy-based approach might thus
433 focus on transmittance, since the transverse lighting used for opacity measurements causes
434 some glare on the shells regardless of condition which may affect the sensitivity of this
435 metric.

436 A loss of transparency could have a negative impact on shelled pteropods since
437 transparency is a form of camouflage in the open ocean environment. Although some
438 pteropod predators, notably the gymnosome (or shell-less) pteropods, are non-visual, the
439 decrease in transparency could potentially serve to increase visibility to visual predators
440 known to feed on pteropods, such as fish and birds (LeBrasseur 1966, Levasseur *et al.*
441 1996, Armstrong *et al.* 2005, Hunt *et al.* 2008, Karnovsky *et al.* 2008, Sturdevant *et al.*
442 2013). It is not known how small of a change in CO₂ concentration will elicit a response in
443 shell condition, but it is noteworthy that changes were evident here in the medium
444 treatment, which in April 2015 was just above an aragonite saturation state of one, a
445 potential environmental threshold. The loss of transparency is likely caused by dissolution
446 of the calcium carbonate matrix, as has been seen at higher resolution using scanning
447 electron microscopy (e.g. Bednaršek *et al.* 2012). It is possible that the more gradual
448 change in CO₂ concentrations that will occur as a result of climate change could allow for
449 adaptation, although shell dissolution has already been documented for wild populations of
450 *L. helicina* exposed to naturally low saturation state conditions (Bednaršek *et al.* 2012,
451 Bednaršek *et al.* 2014). The methods provided here for examining the transparency of

452 shells could be applied to natural populations to look for seasonal and inter-annual
453 changes.

454

455 *Sinking*

456 Although sinking speeds have been previously quantified in some pteropod species
457 (Lalli and Gilmer 1989), the effect of elevated CO₂ on pteropod sinking has not previously
458 been examined, despite the important role that sinking plays in pteropod locomotion and
459 carbonate flux. In this study, the sinking speeds of *L. retroversa* were slower during the
460 second week of exposure to elevated CO₂ and onwards. Measurements of mass made for
461 the April 2015 experiment, normalized to length to account for variability in size, did not
462 indicate a clear pattern among treatments indicative of dissolution due to exposure to
463 enhanced CO₂. It is thus not clear whether the change in sinking speed are due to the shells
464 changing in mass, density, or if they are modified in a way that increases drag. It is also not
465 known whether the experimentally manipulated chemical conditions had any impacts on
466 the mass of the animal bodies, separate from the shells. Given the relatively massive shells
467 and direct linkage between under-saturated conditions and calcium carbonate dissolution,
468 however, it seems likely that changes in sinking speed relate primarily to changes in the
469 shells. The ambient treatment also showed slower sinking with increased duration of
470 exposure, but nonetheless the effect of elevated CO₂ treatment was persistent and sinking
471 both with wings withdrawn and extended showed a similar treatment effect. The decrease
472 in sinking speed for the ambient treatment could indicate a captivity effect, where animals
473 in all treatments might decrease in overall health and vigour with increased duration of
474 time in captivity. It could also be due to removal of larger individuals earlier in the

475 experiments, leading to smaller pteropods being tested in the later weeks, although the
476 effect of exposure on sinking speed was consistent when normalised by the square root of
477 length (based on the observed relationship between size and sinking speed) so this is less
478 likely. In an earlier study, the scaling between shell length and sinking speed for the
479 congeneric species *L. helicina* was between 0.3 and 0.4 (Chang and Yen, 2012), similar to
480 the scaling of 0.5 found in this study. Animal length and speed are also important in
481 determining the Reynolds number (Re). Since *L. retroversa* moves in a transitional regime
482 of Re between ca. 5 and 50, decreases in sinking and swimming speeds might lead to a
483 decrease in Re that could result in increased viscous drag (Walker 2002).

484 Extended wings slowed sinking, presumably as an adaptation to minimise energetic
485 expenditure on swimming to maintain position in the water column. In the laboratory, our
486 observation is that pteropods alternate periods of swimming upwards with sinking, while in
487 the field, the production of mucous webs is thought to slow or even halt sinking, although
488 the prevalence of this behaviour is not well known (Gilmer and Harbison 1986). The bio-
489 energetic consequences to pteropods in the wild of reduced sinking speeds are thus
490 somewhat difficult to assess, but it may be that metabolic costs of maintaining position in
491 the water column are overall reduced under exposure to enhanced CO₂. In contrast,
492 changes in sinking speed may have negative consequences in terms of vulnerability to
493 predation. The gymnosome pteropods feed exclusively on shelled pteropods and for this
494 monospecific predator-prey relationship, withdrawing wings into the shell might make it
495 harder for the predatory shell-less pteropods to successfully capture and consume their
496 prey (Conover and Lalli 1974). Sinking behaviour in the wild is also believed to be a mode
497 of predator avoidance: a response to a disturbance was noted for the pteropod species

498 *Diacria quadridentata*, which withdrew its wings presumably to achieve a faster sinking
499 speed (Gilmer and Harbison 1986). Overall, there are only a few field observations of
500 pteropod behaviour in the wild, but along with the decrease in transparency and
501 camouflage, a decrease in sinking speed with increased CO₂ is another way that *L.*
502 *retroversa* and other shelled pteropods might have increased vulnerability to predators due
503 to ocean acidification.

504 Post-mortem sinking of pteropod shells is important for the biogeochemical cycling
505 of carbon (Berner and Honjo 1981). The solubility of aragonite increases with depth,
506 dropping below a saturation state of one at a depth known as the aragonite compensation
507 depth, which is shoaling due to ocean acidification (Fabry *et al.* 2008). Dissolution is not
508 immediate below the aragonite compensation depth, however, and shells that sink more
509 slowly have more time to be dissolved before reaching deeper water (Byrne *et al.* 1984).
510 The combination of the slower sinking rates observed here with the shoaling of the
511 compensation depth and the elevated rate of dissolution expected from ocean acidification
512 is likely to cause pteropod dissolution and redistribution of carbonate to occur at
513 increasingly shallower depths.

514

515 *Swimming*

516 Although the degradation of the shell after exposure to elevated CO₂ might have
517 been expected to have consequences to the animal's weight and ballast, swimming
518 behaviour did not show clear changes when *L. retroversa* were exposed to elevated CO₂.
519 In particular, unlike sinking speed, swimming speed did not show any clear reduction in
520 the elevated CO₂ treatments. It may be that the differences among the experiments in

521 swimming behaviour and the sensitivity of the various swimming metrics to CO₂ relate to
522 seasonal differences in the overall condition, developmental state, and vigour of the
523 animals prior to capture that persisted through the experiments; these differences may also
524 be influenced by overall low sample sizes. It should also be noted that variability in
525 individual swimming performance may have affected the patterns evident in the April and
526 August 2014 experiments, where multiple animals were present in the filming tank
527 concurrently, relative to the multiple runs done on individual animals in the November
528 2014 and April 2015 experiments. This methodological change was unfortunate and
529 introduces the possibility of pseudo-replication in the earlier two experiments if swimming
530 was observed for the same animal more than once. Given the overall low sample sizes and
531 dearth of previous information, we have presented the observations from both the initial
532 sub-optimal experiments as well as the latter two more rigorous investigations. No
533 consistent differences across the measured swimming metrics were evident associated with
534 the change in method.

535 The significant differences in swimming speed in the first week of exposure may be
536 spurious, as the treatment with the fastest swimmers was not consistent among experiments
537 and significant differences among treatments did not persist after longer exposure
538 durations. A previous study by Manno *et al.* (2012) manipulated CO₂ and salinity to
539 examine how swimming was affected in *L. retroversa* and found that elevated CO₂ alone
540 did not cause a change in swimming speed or wing beat frequency after eight days of
541 exposure, while decreased salinity combined with increased CO₂ conditions slowed the
542 swimming and increased the beat frequency. This supports the idea that our findings at one
543 week are spurious.

544 More consistent in the present study than the patterns in swimming speed was a
545 trend towards decreased wing beat frequency in the medium and high treatments relative to
546 ambient, albeit only significant in one of the experiments. This reduction in wing beat
547 frequency is interesting in its not being accompanied by an associated difference between
548 treatments in swimming speed (although at the individual level, wing beat frequency was
549 positively correlated with swimming speed). A reduction in beat frequency may suggest a
550 reduced metabolic cost of swimming in the animals exposed to elevated CO₂, and is
551 perhaps associated with a less massive shell. While there was not a good correlation
552 between swimming speed and length, there was a significant negative correlation between
553 wing beat frequency and length, which has also been noted in another study where larger
554 *L. helicina* beat their wings less frequently but achieved greater speeds (Chang and Yen
555 2012). That more detailed study of swimming kinetics also found that across sizes the
556 trajectory and timing of the wing strokes varied, possibly as a response to changing
557 Reynolds number regimes.

558 Tortuosity often, but not always, showed differences associated with treatment in
559 the present study, with greatest tortuosity in the ambient treatment. Tortuosity was
560 significantly negatively correlated to swimming speed, as animals tended to exhibit more
561 horizontal movements that often appeared helical in nature when swimming at lower
562 speeds. Tortuosity and length were also negatively related, though not quite significantly.
563 Chang and Yen (2012) similarly found that the helical component of *L. helicina* swimming
564 paths was greater for larger individuals. Pteropod swimming relies on the rotation of the
565 shell between the power and recovery strokes and differential dissolution along the
566 elongate shells of individual *L. retroversa* could conceivably influence swimming

567 efficiency. Examining the asymmetry in swimming speed induced by the power and
568 recovery strokes, however, did not show any effect of CO₂ exposure. In general it is
569 possible that the limited effects observed on the swimming metrics examined here in
570 relation to CO₂ exposure are due to shell dissolution (and associated potential impacts on
571 weight and ballast) not being advanced enough to result in discernible consequences to
572 swimming. If future studies can overcome limitations in the durations over which
573 pteropods can be maintained in captivity, the longer-term effects on locomotion of
574 enhanced CO₂ might be examined.

575

576 **Conclusions**

577 This study observed decreased sinking speeds in pteropods exposed to conditions
578 of elevated CO₂ that could exist by the end of the century, suggesting that ocean
579 acidification could affect pteropod fitness, as sinking is a mode of predator avoidance.
580 Decreased sinking speeds will likely also slow the passive transport of calcium carbonate
581 to depth. Ocean acidification could potentially also increase the visibility of pteropods to
582 predators, since increased CO₂ significantly affected the transparency of shells. Longer
583 perturbation experiments or greater replication may be needed to understand whether
584 ocean acidification affects swimming. The cues that pteropods respond to that motivate
585 their upward swimming are not known, and whether these cues are influenced by CO₂
586 treatment is also uncertain. Overall, more behavioural experiments on pteropods are
587 needed to understand the consequences of ocean acidification, although this relies on the
588 development of improved culture techniques in order to achieve adequately large sample
589 sizes and to examine impacts over longer time periods (Howes *et al.* 2015).

590

591 **Supplementary Materials**

592 Supplementary material is available at ICES JMS online, including figures of shell mass
593 measurements normalized to length vs. exposure duration for the April 2015 experiment
594 and swimming speed vs. length as well as a table providing the full carbonate chemistry
595 measurements and calculations. MATLAB code for the analysis of pteropod shell
596 transmittance and opacity is available at <http://www.bco-dmo.org/project/2263>.

597

598 **Acknowledgements**

599 We would like to thank Captain K. Houtler and Mate I. Hanley of the R/V *Tioga*
600 for their efforts that allowed us to collect the necessary number of pteropods. We
601 appreciate the help we received at sea and in the lab collecting and rearing the pteropods
602 from P. Alatalo, L. Blanco Bercial, S. Chu, N. Copley, T. Crockford, S. Crosby, M.
603 Edenius, K. Hoering, R. Levine, M. Lowe, C. Pagniello, A. Schlunk, A. Tarrant, A.
604 Thabet, T. White and P. Wiebe. We thank R. Galat and D. McCorkle for their help setting
605 up the CO₂ exposure system and S. Chu, K. Hoering, K. Morkeski, and Z. Sandwich for
606 their invaluable help measuring carbonate chemistry. K. Young provided much appreciated
607 analysis code for filming. We also thank S. Colin, J. Costello, H. Jiang, and L. Mullineaux
608 for loaning equipment used for filming. We thank C. Ashjian and two anonymous
609 reviewers for providing helpful comments on manuscript drafts. Funding for this research
610 was provided by a National Science Foundation grant to Lawson, Maas, and Tarrant
611 (OCE-1316040). Additional support for field sampling was provided by the WHOI Coastal

612 Ocean Institute, Pickman Foundation, and the Tom Haas Fund at the New Hampshire
613 Charitable Foundation.

614

615 **References**

616

617 Ackman, R.G., Hingley, J., and MacKay, K.T. 1972. Dimethyl sulfide as an odor component in Nova Scotia
618 fall mackerel. *Journal of Fisheries Research Board of Canada*. 29: 1085-1088.

619 Almogi-Labin, A., Luz, B., Duplessy, J.-C. 1986. Quaternary paleo-oceanography, pteropod preservation and
620 stable-isotope record of the Red Sea. *Palaeogeography, Palaeoclimatology, Palaeoecology*. 57:
621 195-211.

622 Armstrong, J.L., Boldt, J.L., Cross, A.D., Moss, J.H., Davis, N.D., Meyers, K.W., Walker, R.V., *et al.* 2005.
623 Distribution, size, and interannual, seasonal and diel food habits of northern Gulf of Alaska juvenile
624 pink salmon, *Oncorhynchus gorbuscha*. *Deep-Sea Research II: Tropical Studies in Oceanography*.
625 52: 247-265.

626 Bednaršek, N., Tarling, G.A., Bakker, D.C., Fielding, S., Jones, E.M., Venables, H.J., Ward, P., *et al.* 2012.
627 Extensive dissolution of live pteropods in the Southern Ocean. *Nature Geoscience*. 5: 881-885.

628 Bednaršek, N., Feely, R.A., Reum, J.C.P., Peterson, B., Menkel, J., Alin, S.R., and Hales, B. 2014. *Limacina*
629 *helicina* shell dissolution as an indicator of declining habitat suitability owing to ocean acidification
630 in the California Current Ecosystem. *Proceedings of the Royal Society B*. 281: 20140123.

631 Bednaršek, N., and Ohman, M.D. 2015. Changes in pteropod distributions and shell dissolution across a
632 frontal system in the California Current System. *Marine Ecology Progress Series*. 523: 93-103.

633 Berner, R.A., and Honjo, S. 1981. Pelagic sedimentation of aragonite: its geochemical significance. *Science*.
634 211(4485): 940-942.

635 Busch, D.S., Maher, M., Thibodeau, P., and McElhany, P. 2014. Shell condition and survival of Puget Sound
636 pteropods are impaired by ocean acidification conditions. *PLoS ONE*. 9(8): e105884. doi:
637 10.1371/journal.pone.0105884.

638 Byrne, R.H., Acker, J.G., Betzer, P.R., Feely, R.A., and Cates, M.H. 1984. Water column dissolution of
639 aragonite in the Pacific Ocean. *Nature*. 312: 322-326.

640 Chan, K.Y.K., Grünbaum, D., and O'Donnell, M.J. 2011. Effects of ocean acidification induced
641 morphological changes on larval swimming and feeding. *The Journal of Experimental Biology*. 214:
642 3857-3867.

643 Chang, Y., and Yen, J. 2012. Swimming in the intermediate Reynolds range: kinematics of the pteropod
644 *Limacina helicina*. *Integrative and Comparative Biology*. 52(5): 597-615.

645 Comeau, S., Gorsky, G., Jeffree, R., Teysse, J.L., and Gattuso, J.P. 2009. Key arctic pelagic mollusk
646 (*Limacina helicina*) threatened by ocean acidification. *Biogeosciences*. 6: 1877-1882.

647 Comeau, S., Jeffree, R., Teysse, J.L., and Gattuso, J.P. 2010. Response of the Arctic pteropod *Limacina*
648 *helicina* to projected future environmental conditions. *PLoS ONE*. 5(6): e11362. doi:
649 10.1371/journal.pone.0011362.

650 Comeau, S., Alliouane, S., and Gattuso, J.P. 2012. Effects of ocean acidification on overwintering juvenile
651 Arctic pteropods *Limacina helicina*. *Marine Ecology Progress Series*. 456: 279-284.

652 Conover, R.J., and Lalli, C.M. 1974. Feeding and growth in *Clione limacina* (Phipps), a pteropod mollusk. II.
653 Assimilation, metabolism, and growth efficiency. *Journal of Experimental Marine Biology and*
654 *Ecology*. 16: 131-154.

655 Dickson, A.G., and Millero, F.J. 1987. A comparison of the equilibrium constants for the dissociation of
656 carbonic acid in seawater media. *Deep Sea Research*. 34: 1733-1743.

- 657 Dickson, A.G. 1990. Thermodynamics of the dissociation of boric acid in synthetic seawater from 273.15 to
658 318.15 K. *Deep Sea Research*. 37: 755-766.
- 659 Fabry, V.J., Seibel, B.A., Feely, R.A., and Orr, J.C. 2008. Impacts of ocean acidification on marine fauna and
660 ecosystem processes. *ICES Journal of Marine Science*. 65: 414 -432.
- 661 Gilmer, R.W., and Harbison, G.R. 1986. Structure and field behavior of pteropod molluscs: feeding methods
662 in the families Cavoliniidae, Limacinidae, and Peraclididae (Gastropoda: Thecosomata). *Marine*
663 *Biology*. 91: 47-57.
- 664 Haddad, G.A., and Droxler, A.W. 1996. Metastable CaCO₃ dissolution at intermediate water depths of the
665 Caribbean and western North Atlantic: Implications for intermediate water circulation during the
666 past 200,000 years. *Paleoceanography*. 11(6): 701-716.
- 667 Hunt, B.P.V., Pakhomov, E.A., Hosie, G.W., Siegel, V., Ward, P., and Bernard, K. 2008. Pteropods in the
668 southern ocean ecosystems. *Progress in Oceanography*. 78: 193-221.
- 669 Karnovsky, N.J., Hobson, K.A., Iverson, S., and Hunt, G.L. 2008. Seasonal changes in diets of seabirds in
670 the North Water Polynya: a multiple-indicator approach. *Marine Ecology Progress Series*. 357: 291-
671 299.
- 672 Lalli, C.M., and Gilmer, R.W. 1989. Pelagic snails: the biology of holoplanktonic gastropod mollusks.
673 *Stanford University Press*, Los Altos. 259 pp.
- 674 LeBrasseur, R.J. 1966. Stomach contents of salmon and steelhead trout in the Northeastern Pacific Ocean.
675 *Journal of Fisheries Research Board of Canada*. 23(1): 85-100.
- 676 Levasseur, M., Keller, M.D., Bonneau, E., D'Amours, D., and Bellows, W.K. 1994. Oceanographic basis of
677 a DMS-related Atlantic cod (*Gadus morhua*) fishery problem: blackberry feed. *Canadian Journal of*
678 *Fisheries and Aquatic Sciences*. 51: 881-889.
- 679 Lischka, S., Büdenbender, J., Boxhammer, T., and Riebesell, U. 2011. Impact of ocean acidification and
680 elevated temperatures on early juveniles of the polar shelled pteropod *Limacina helicina*: mortality,
681 shell degradation, and shell growth. *Biogeosciences*. 8: 919-932.
- 682 Lischka, S., and Riebesell, U. 2012. Synergistic effects of ocean acidification and warming on overwintering
683 pteropods in the Arctic. *Global Change Biology*. 18: 3517-3528.
- 684 Maas, A.E., Wishner, K.F., and Seibel, B.A. 2012. Metabolic suppression in thecosomatous pteropods as an
685 effect of low temperature and hypoxia in the eastern tropical North Pacific. *Marine Biology*. 159:
686 1955-1967.
- 687 Manno, C., Morata, N., and Primicerio, R. 2012. *Limacina retroversa*'s response to combined effects of
688 ocean acidification and sea water freshening. *Estuarine, Coastal and Shelf Science*. 113: 163-171.
- 689 Mehrbach, C., Culberson, C.H., Hawley, J.E., and Pytkowicz, R.M. 1973. Measurement of apparent
690 dissociation constants of carbonic acid in seawater at atmospheric pressure. *Limnology and*
691 *Oceanography*. 18: 897-907.
- 692 Murphy, D.W., Adhikari, D., Webster, D.R., and Yen, J. 2016. Underwater flight by the planktonic sea
693 butterfly. *Journal of Experimental Biology*. 219: 535-543.
- 694 Orr, J.C., Fabry, V.J., Aumont, O., Bopp, L., Doney, S.C., Feely, R.A., and Gnanadesikan, A., *et al.* 2005.
695 Anthropogenic ocean acidification over the twenty-first century and its impacts on calcifying
696 organism. *Nature*. 437(29): 681-686.
- 697 Owen, J.P., and Ryu, W.S. 2015. The effects of linear and quadratic drag on falling spheres: an
698 undergraduate laboratory. *European Journal of Physics*. 26: 1085-1091.
- 699 Pakhomov, E.A., Perissinotto, R., and McQuaid, C.D. 1996. Prey composition and daily rations of myctophid
700 fishes in the Southern Ocean. *Marine Ecology Progress Series*. 134: 1-14.

- 701 Pierrot, D., Lewis, E., and Wallace, D. 2006. Co2sys DOS Program developed for CO₂ system calculations.
702 Carbon Dioxide Information anlysis Center, Oak Ridge National Laboratory, US Department of
703 Energy ORNL/CDIAC-105.
- 704 Pomerleau, C., Lesage, V., Ferguson, S.H., Winkler, G., Petersen, S.D., and Higdon, J.W. 2012. Prey
705 assemblage isotopic variability as a tool for assessing diet and the spatial distribution of bowhead
706 whale *Balaena mysticetus* foraging in the Canadian eastern Arctic. *Marine Ecology Progress Series*.
707 469: 161-174.
- 708 Royal Society. 2005. Ocean acidification due to increasing atmospheric carbon dioxide. *Policy Document*
709 *12/05, The Royal Society*.
- 710 Sabine, C.L., Feely, R.A., Gruber, N., Key, R.M., Lee, K., Bullister, J.L., Wanninkhof, R., *et al.* 2004. The
711 oceanic sink for anthropogenic CO₂. *Science*. 305(5682): 367-371.
- 712 Sturdevant, M.V., Orsi, J.A., and Fergusson, E.A. 2013. Diets and trophic linkages of epipelagic fish
713 predators in coastal Southeast Alaska during a period of warm and cold climate years, 1997-2011.
714 *Marine and Coastal Fisheries: Dynamics, Management, and Ecosystem Science*. 4: 526-545.
- 715 Thabet, A.A., Maas, A.E., Lawson, G.L., and Tarrant, A.M. 2015. Life cycle and early development of the
716 thecosomatous pteropod *Limacina retroversa* in the Gulf of Maine, including the effect of elevated
717 CO₂ levels. *Marine Biology*. 162: 2235-2249.
- 718 Walker, J.A. 2002. Functional Morphology and Virtual Models: Physical Constraints on the Design of
719 Oscillating Wings, Fins, Legs, and Feed at Intermediate Reynolds Numbers. *Integrative and*
720 *Comparative Biology*. 42: 232-242.
- 721 Wall-Palmer, D., Smart, C.W., and Hart, M.B. 2013. In-life pteropod shell dissolution as an indicator of past
722 ocean carbonate saturation. *Quaternary Science Reviews*. 81: 29-34.
- 723 Wanninkhof, R., Barbero, L., Byrne, R., Cai, W.J., Huang, W.J., Zhang, J.Z., Baringer, M., and Langdon, C.
724 2015. Ocean acidification along the Gulf Coast and East Coast of the USA. *Continental Shelf*
725 *Resesarch*. 98: 54-71.
- 726 Wang, Z.A., and Cai W.J. 2004. Carbon dioxide degassing and inorganic carbon export from a marsh-
727 dominated estuary (the Duplin River): a marsh CO₂ pump. *Limnology and Oceanography*. 49: 341-
728 354.
- 729 Wang, Z.A., Wanninkhof, R., Cai, W.J., Byrne, R.H., Hu, X., Peng, T.H., and Huang, H.J. 2013. The marine
730 inorganic carbon system along the Gulf of Mexico and Atlantic coasts of the United States: insights
731 from transregional coastal carbon study. *Limnology and Oceanography*. 58(1): 325-342.
- 732 Wheeler, J.D., Helfrich, K.R., Anderson, E.J., McGann, B., Staats, P., Wargula, A.E., Wilt, K., and
733 Mullineaux, L.S. 2013. Upward swimming of competent oyster larvae *Crassostrea virginica* persists
734 in highly turbulent flow as detected by PIV flow subtraction. *Marine Ecology Progress Series*. 488:
735 171-185.
- 736 Wormuth, J.H. 1981. Vertical distributions and diel migrations of *Euthecosomata* in the northwest Sargasso
737 Sea. *Deep-sea Research*. 28A(12): 1493-1515.
- 738

739 **Captions**

740 Figure 1. (a) Schematic of the filming set up. The seawater tank had a mirror to show the
741 actual and reflected image of an animal sinking or swimming, allowing position to be
742 determined in three dimensions. A high speed camera was used for filming and
743 illumination was provided by an LED panel. The tank was 10 cm long, 10 cm wide, and 10
744 cm high. (b) Filming set up showing the mirrored tank with the fixed pipette that was used
745 to drop the pteropods through for sinking trials. (c) One frame of a video shows the actual
746 image and mirrored image of a sinking pteropod with wings withdrawn, shortly after
747 exiting the fixed pipette.

748

749 Figure 2. (a) Speed vs time plot of a swimming trial, showing the full time-series of speed
750 from the 3 second video segment (blue), along with calculated mean speed (red line), a
751 wing beat period, and the asymmetry in peaks. The wing beat frequency was calculated as
752 $1/(\text{beat period})$ and included both the power and recovery strokes. Power strokes were
753 consistently associated with greater speeds and asymmetry between the peak speeds of the
754 power and recovery stroke was measured as the difference between subsequent peaks of
755 speed divided by the larger of the two. (b) The 3D trajectory of a swimming *L. retroversa*
756 shows the pattern of motion. Note that this is a scatter plot but the high frame rate of the
757 camera leads to the points appearing essentially as a line. Tortuosity was calculated as the
758 total cumulative distance traveled divided by the direct distance from starting point to
759 finish.

760

761 Figure 3. (a) Transmittance (proportion of transmitted light) and (b) opacity (proportion of
762 reflected light) of *L. retroversa* shells from the April 2015 experiment relative to duration
763 of exposure for each of the three CO₂ treatments.

764

765 Figure 4. (a) Terminal sinking speed for *L. retroversa* with wings withdrawn for the four
766 experiments (circle: April 2014; square: August 2014; diamond: November 2014; triangle:
767 April 2015) after durations of exposure of 1-4 weeks. From left to right within each weekly
768 bracket the ambient, medium, and high treatment are plotted, although the treatments were
769 measured together of the course of 2-5 days and are spaced along the x-axis simply for
770 easier visualisation. The error bars denote standard error. (b) The terminal sinking speed
771 with wings extended for the April 2014, August 2014, and November 2015 experiments.
772 No measurements of sinking with wings extended were made in April 2015 or in week 3 of
773 any of the experiments.

774

775 Figure 5. Log₁₀ terminal sinking speed with wings withdrawn vs log₁₀ shell length for each
776 treatment (points) along with a linear regression for each treatment (lines). The slope of the
777 linear regressions shows the power scaling between sinking speed and shell length.

778 Contours of constant Reynolds numbers (Re) of 5, 10, and 20 are shown in black.

779

780 Figure 6. (a) Mean swimming speed, (b) wing beat frequency, and (c) tortuosity for *L.*
781 *retroversa* for the four experiments (circle: April 2014; square: August 2014; diamond:
782 November 2014; triangle: April 2015) after durations of exposure of 1-3 weeks. From left
783 to right within a week the ambient, medium, and high treatment are plotted, although


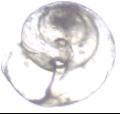
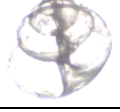

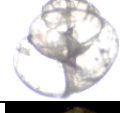

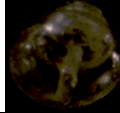
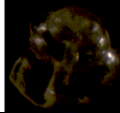
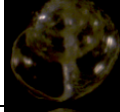
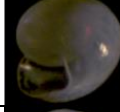
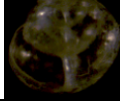

784 treatments were measured together over the course of 2-5 days. The error bars denote
785 standard error. Both the power and recovery stroke are included in each wing beat in
786 calculating wing beat frequency.
787

788 Table 1. The carbonate chemistry parameters partial pressure of CO₂ (pCO₂), pH, and aragonite saturation
 789 state (Ω_A) are average values for the water leaving the treatment carboys at days 7 and 14 during water
 790 changes. TA and DIC were directly measured and were used for calculation of the other parameters.
 791 Measurements of ingoing water at the start of each week of exposure in April and August 2014 appeared to
 792 indicate insufficient pre-equilibration, although target levels were reached by day 1 (see text and
 793 Supplementary Table S1). The values are reported as the mean \pm standard deviation.
 794

Experiment	Treatment	pCO ₂ (μ atm)	pH	Ω_A
April 2014	Ambient	470 \pm 20	7.96 \pm 0.02	1.54 \pm 0.06
	Medium	850 \pm 40	7.73 \pm 0.02	0.94 \pm 0.03
	High	1190 \pm 120	7.59 \pm 0.04	0.70 \pm 0.07
Aug 2014	Ambient	440 \pm 40	7.98 \pm 0.03	1.58 \pm 0.11
	Medium	650 \pm 170	7.84 \pm 0.11	1.21 \pm 0.30
	High	990 \pm 100	7.66 \pm 0.04	0.80 \pm 0.08
Nov 2014	Ambient	480 \pm 50	7.95 \pm 0.04	1.49 \pm 0.11
	Medium	1100 \pm 290	7.63 \pm 0.10	0.76 \pm 0.15
	High	1320 \pm 160	7.55 \pm 0.05	0.63 \pm 0.07
April 2015	Ambient	440 \pm 30	7.99 \pm 0.03	1.61 \pm 0.09
	Medium	740 \pm 100	7.78 \pm 0.05	1.05 \pm 0.12
	High	1180 \pm 190	7.59 \pm 0.07	0.70 \pm 0.11

795

796 Table 2. Representative images showing the changes in
 797 shell appearance from day 2 to day 15 for each treatment
 798 during the April 2015 experiment. Transmittance images
 799 are taken when light is shining from below the sample,
 800 and opacity images are taken when light is illuminating
 801 the sample from the sides.
 802

	Treatment	Day 2	Day 15
Transmittance	Ambient		
	Medium		
	High		
Opacity	Ambient		
	Medium		
	High		

803
 804

805 Table 3. Cruise and experiment details and associated statistics. For each type of observation of *L. retroversa* (shell condition, sinking, or swimming) and each
 806 duration of exposure the sample sizes are listed (ambient, medium, high). Test statistics (F for one-way ANOVAs and H for Kruskal-Wallis one-way ANOVAs
 807 on ranks) are reported for comparisons among treatments for multiple sinking, swimming, and shell variables abbreviated as follows: “Sinking wings in” is
 808 sinking speed with wings withdrawn, “Sinking wings out” is sinking speed with wings extended, “Swim speed” is mean swimming speed, “Beat” is wing beat
 809 frequency, and “Tort” is tortuosity. * p<0.05, ** p<0.01, *** p<0.001, NS=Non-Significant
 810
 811

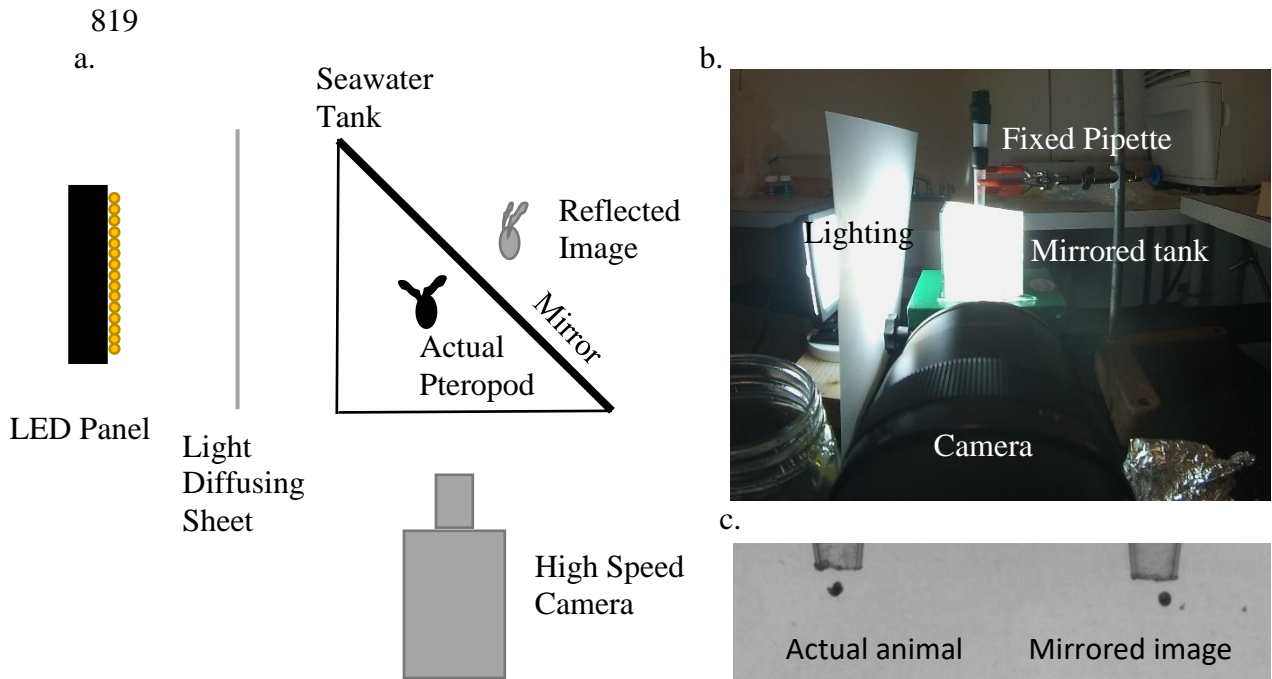
Experiment	Cruise Dates	Type of Observation	Exposure Duration	Sample Size Amb., Med., High	One-way ANOVA: F Kruskal-Wallis one-way ANOVA: H
April 2014	25 April – 27 April 2014	Sinking	4 Weeks	10, 10, 7	Sinking wings in: F=9.8***; Sinking wings out: F=9.0**
		Swimming	3 Weeks	11, 7, 10	Swim speed: F=0.9 ^{NS} , Beat: H=1.7 ^{NS} , Tort: H=8.4*
August 2014	19 August 2014	Sinking	1 Week	10, 12, 13	Sinking wings in: H=1.1 ^{NS} , Sinking wings out: F=1.0 ^{NS}
		Swimming	1 Week	13, 21, 17	Swim speed: F=4.6*, Beat: H=2.1 ^{NS} , Tort: H=10.6**
November 2014	4 November – 6 November 2014	Sinking	1 Week	20, 22, 20	Sinking wings in: F=0.3 ^{NS} , Sinking wings out: F=0.4 ^{NS}
		Sinking	2 Weeks	25, 20, 18	Sinking wings in : F=4.2*, Sinking wings out : F=6.4**
		Swimming	2 Weeks	3, 10, 10	Speed: H=1.6 ^{NS} , Beat: F=1.6 ^{NS} , Tort: H=2.3 ^{NS}
April 2015	26 April – 27 April 2015	Sinking	1 Week	25, 26, 25	Sinking wings in: F=5.8**
		Sinking	2 Weeks	26, 26, 22	Sinking wings in: H=11.6**
		Sinking	3 Weeks	26, 22, 16	Sinking wings in: F=19.0***
		Swimming	1 Week	15, 18, 16	Swim speed: F=3.7*, Beat: F=9.5***, Tort: H=4.7 ^{NS}
		Swimming	2 Weeks	8, 14, 18	Swim speed: F=0.1 ^{NS} , Beat: F=1.5 ^{NS} , Tort: H=5.1 ^{NS}
		Shells	2 Days	8, 9, 8	Transmittance: F=0.1 ^{NS} , Opacity: H=0.8 ^{NS}
		Shells	4 Days	8, 8, 8	Transmittance: H=9.0*, Opacity: H=8.1*
		Shells	8 Days	8, 7, 5	Transmittance: H=14.5***, Opacity: H=13.0**
Shells	15 Days	7, 7, 5	Transmittance: F=60***, Opacity: F=212***		

812 Table 4. Correlation coefficients (r) among the swimming variables: mean swimming speed, wing beat
 813 frequency, path tortuosity, and asymmetry between the peaks of speed (i.e. the difference between the power
 814 and recovery stroke). Bold indicates significant correlations. * p<0.05, ** p<0.01, *** p<0.001, NS=Non-
 815 Significant

Correlation coefficient	Length	Wing Beat frequency	Tortuosity	Asymmetry in peaks
Speed	0.0005 ^{NS}	0.2395 ***	-0.4357 ***	-0.18233 *
Length		-0.3785 ***	-0.1418 ^{NS}	0.110331 ^{NS}
Wing Beat			0.1209 ^{NS}	-0.13198 ^{NS}
Tortuosity				0.059909 ^{NS}

816
817

818



820

821

822

823

824

825

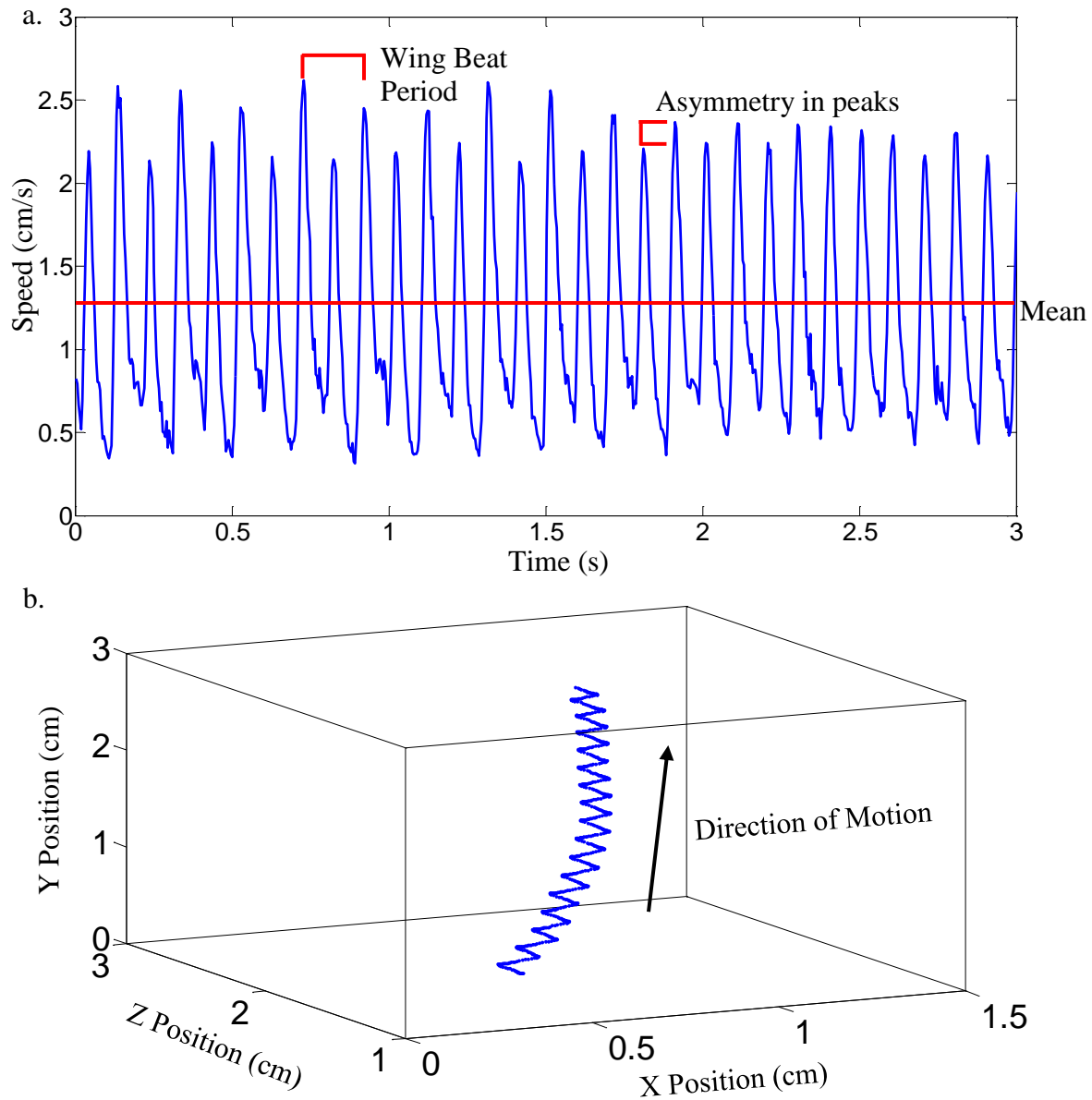
826

827

828

Figure 1. (a) Schematic of the filming set up. The seawater tank had a mirror to show the actual and reflected image of an animal sinking or swimming, allowing position to be determined in three dimensions. A high speed camera was used for filming and illumination was provided by an LED panel. The tank was 10 cm long, 10 cm wide, and 10 cm high. (b) Filming set up showing the mirrored tank with the fixed pipette that was used to drop the pteropods through for sinking trials. (c) One frame of a video shows the actual image and mirrored image of a sinking pteropod with wings withdrawn, shortly after exiting the fixed pipette.

829



830

831

832 Figure 2. (a) Speed vs time plot of a swimming trial, showing the full time-series of speed from the 3 second

833 video segment (blue), along with calculated mean speed (red line), a wing beat period, and the asymmetry in

834 peaks. The wing beat frequency was calculated as $1/(\text{beat period})$ and included both the power and recovery

835 strokes. Power strokes were consistently associated with greater speeds and asymmetry between the peak

836 speeds of the power and recovery stroke was measured as the difference between subsequent peaks of speed

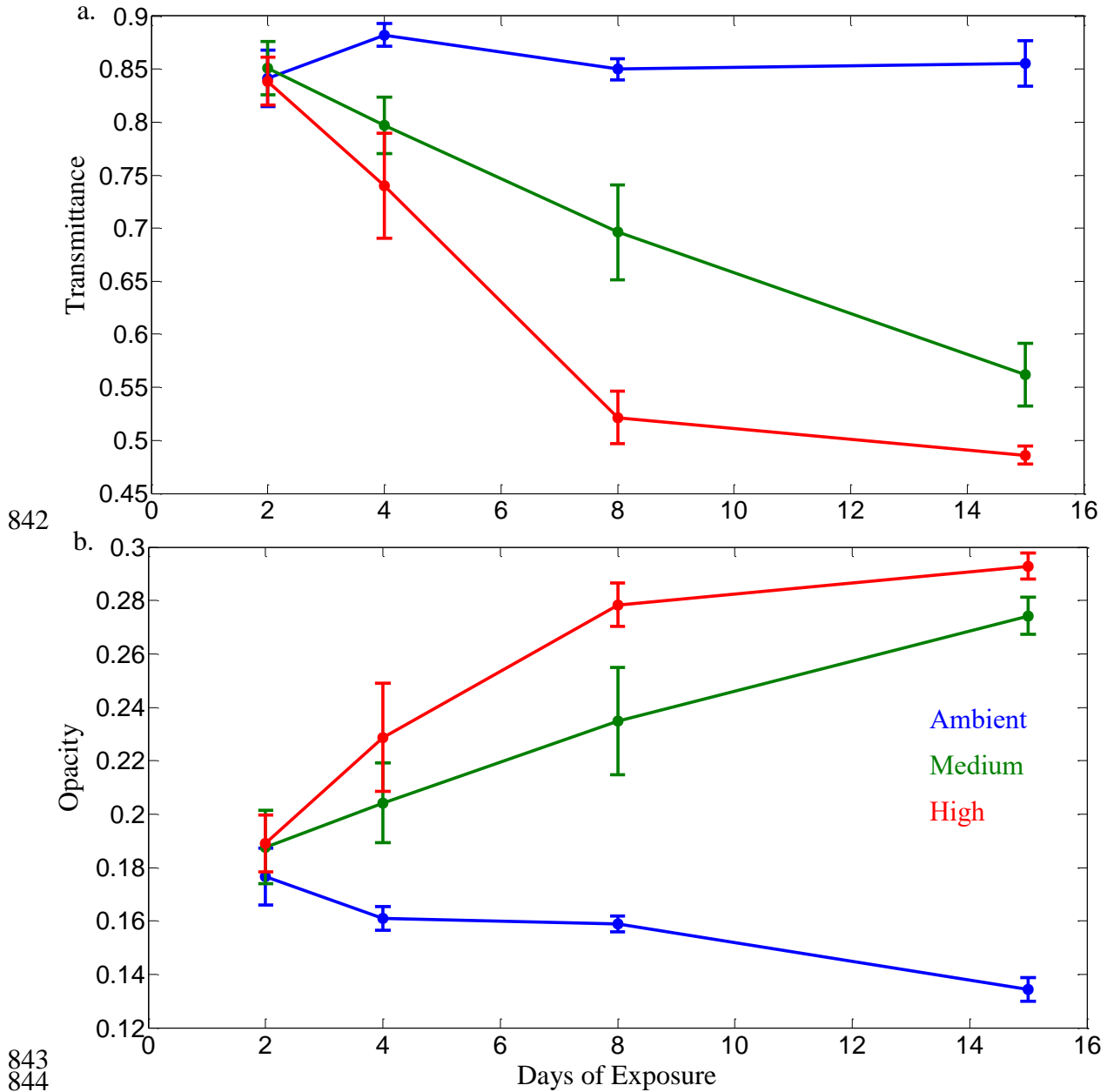
837 divided by the larger of the two. (b) The 3D trajectory of a swimming *L. retroversa* shows the pattern of

838 motion. Note that this is a scatter plot but the high frame rate of the camera leads to the points appearing

839 essentially as a line. Tortuosity was calculated as the total cumulative distance traveled divided by the direct

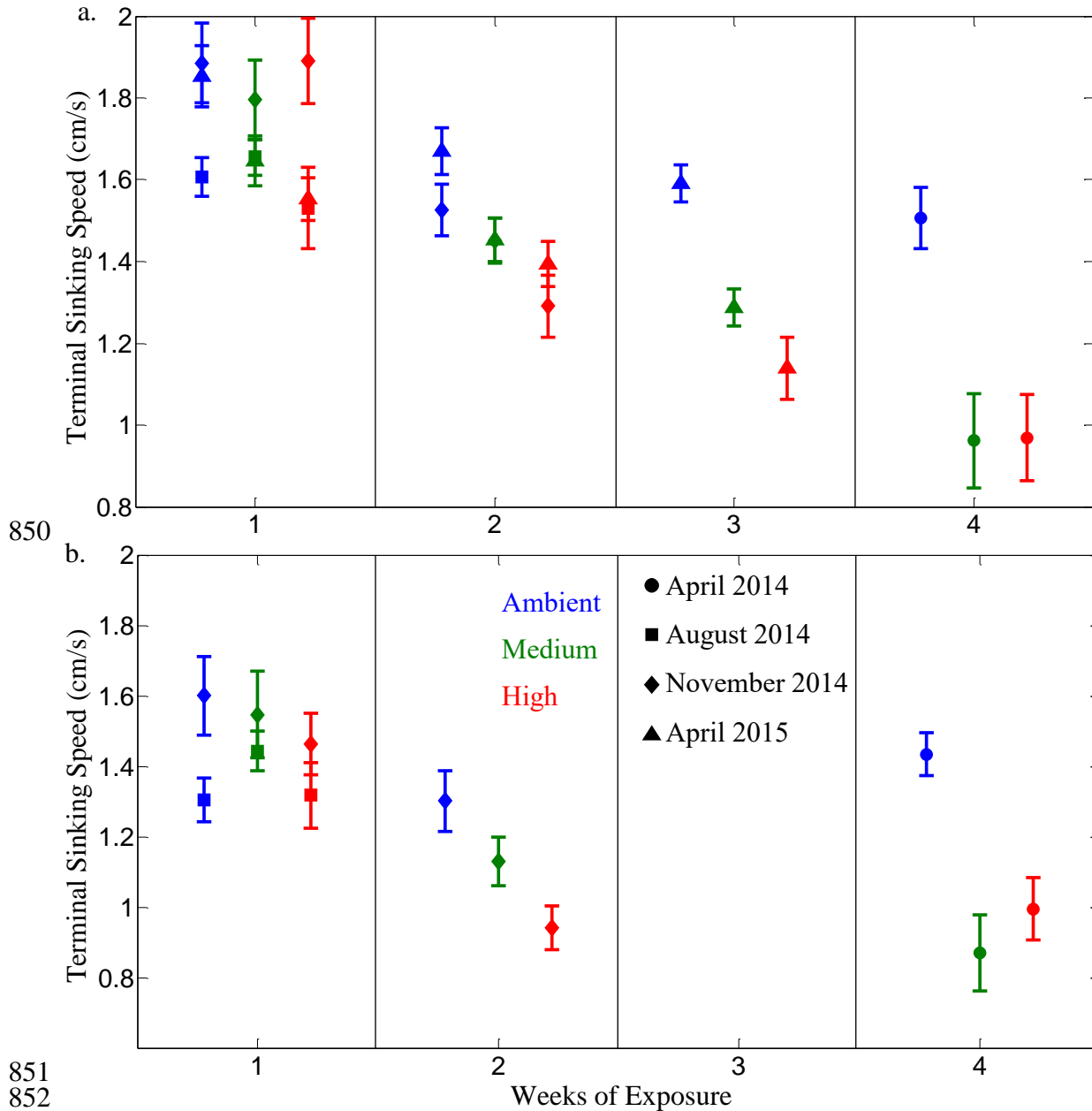
840 distance from starting point to finish.

841



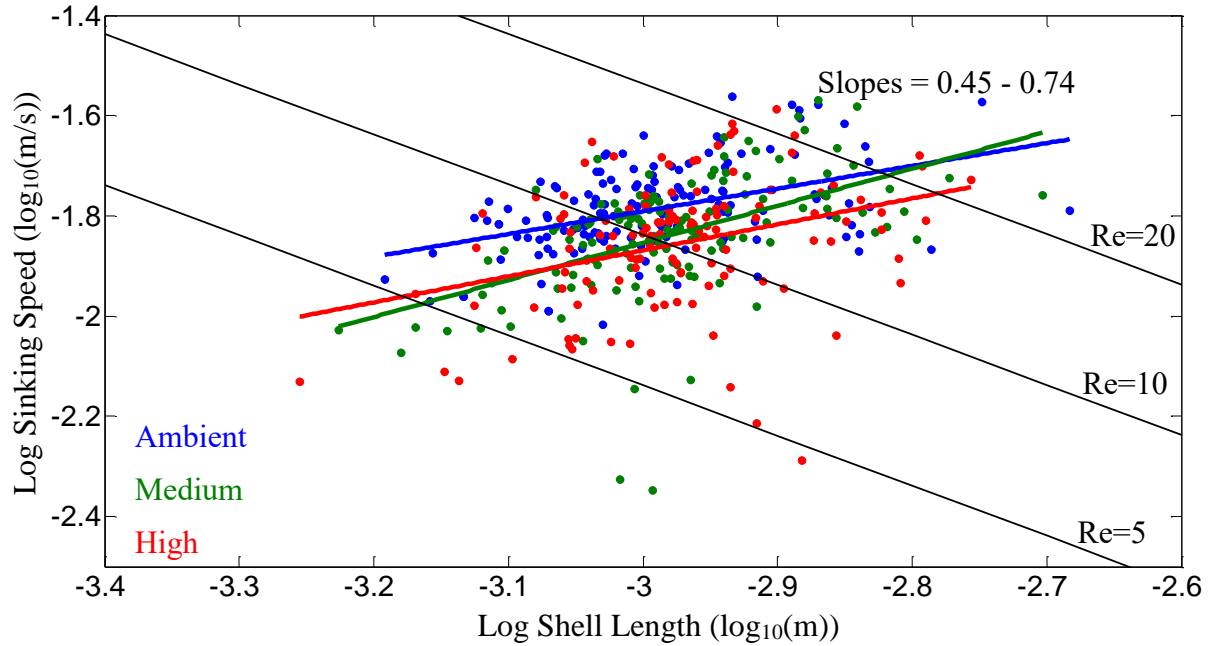
843
844
845
846
847
848
849

Figure 3. (a) Transmittance (proportion of transmitted light) and (b) opacity (proportion of reflected light) of *L. retroversa* shells from the April 2015 experiment relative to duration of exposure for each of the three CO₂ treatments.



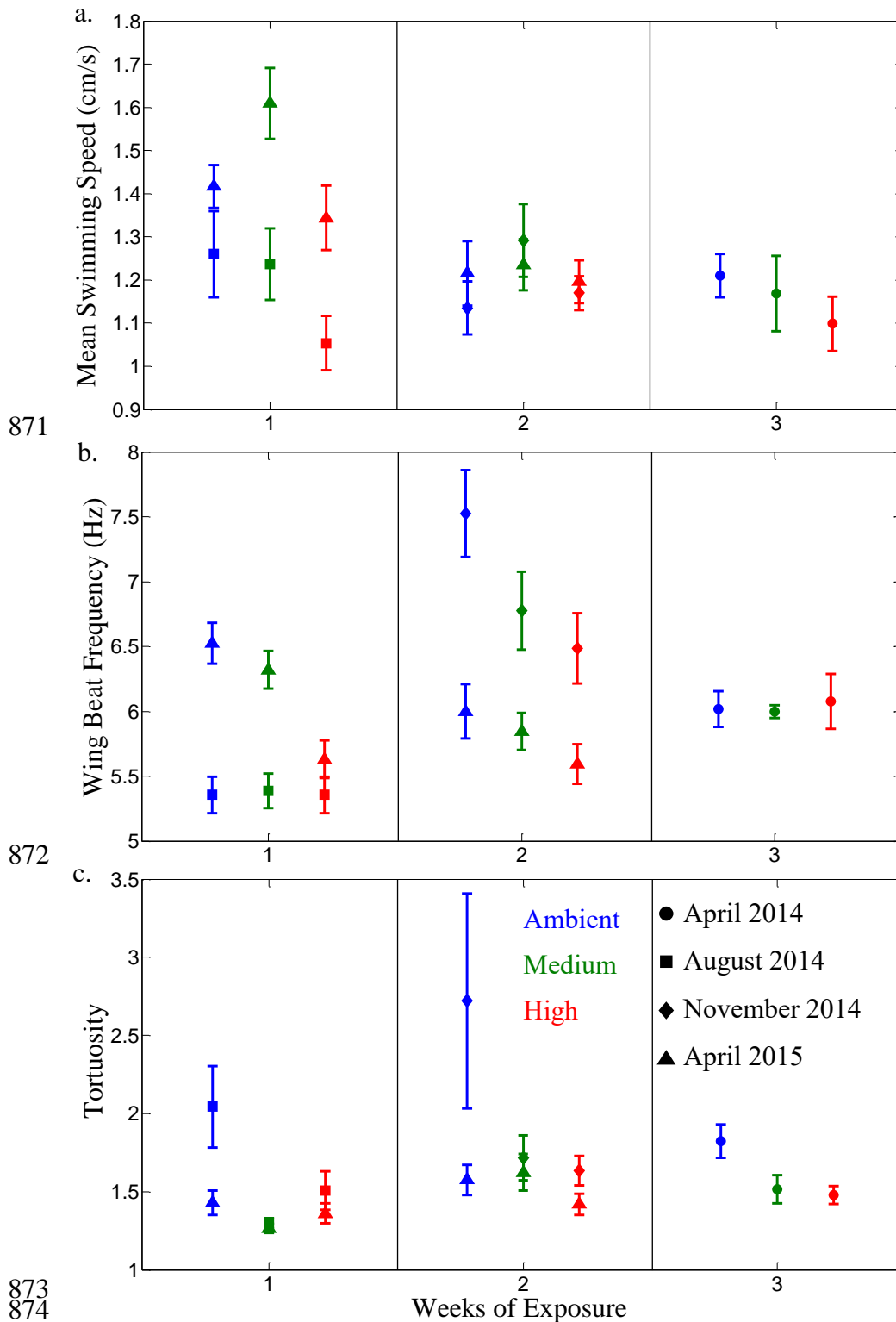
851
852
853
854
855
856
857
858
859
860
861
862

Figure 4. (a) Terminal sinking speed for *L. retroversa* with wings withdrawn for the four experiments (circle: April 2014; square: August 2014; diamond: November 2014; triangle: April 2015) after durations of exposure of 1-4 weeks. From left to right within each weekly bracket the ambient, medium, and high treatment are plotted, although the treatments were measured together of the course of 2-5 days, and are spaced along the x-axis simply for easier visualisation. The error bars denote standard error. (b) The terminal sinking speed with wings extended for the April 2014, August 2014, and November 2015 experiments. No measurements of sinking with wings extended were made in April 2015 or in week 3 of any of the experiments.



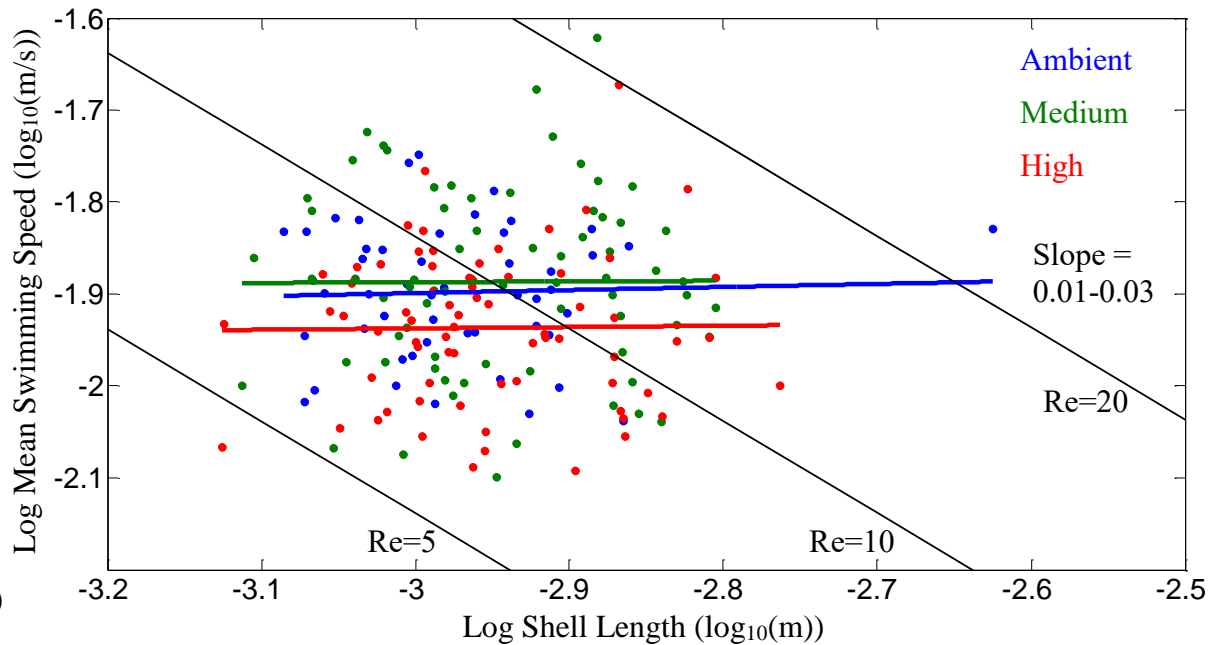
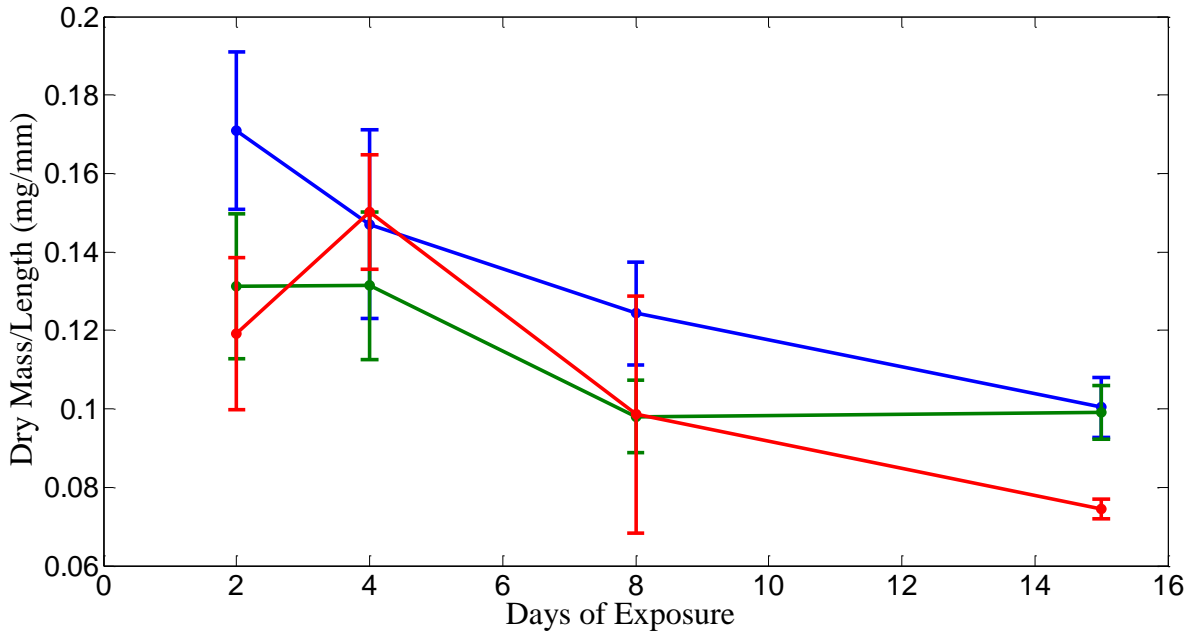
863
864
865
866
867
868
869
870

Figure 5. \log_{10} terminal sinking speed with wings withdrawn vs \log_{10} shell length for each treatment (points) along with a linear regression for each treatment (lines). The slope of the linear regressions shows the power scaling between sinking speed and shell length. Contours of constant Reynolds numbers (Re) of 5, 10, and 20 are shown in black.



875 Figure 6. (a) Mean swimming speed, (b) wing beat frequency, and (c) tortuosity for *L. retroversa* for the four
 876 experiments (circle: April 2014; square: August 2014; diamond: November 2014; triangle: April 2015) after
 877 durations of exposure of 1-3 weeks. From left to right within a week the ambient, medium, and high
 878 treatment are plotted, although treatments were measured together over the course of 2-5 days. The error bars
 879 denote standard error. Both the power and recovery stroke are included in each wing beat in calculating wing
 880 beat frequency.

881 **Supplementary Materials**
882



898 Supplemental Table S1. Carbonate chemistry parameters measured and calculated over the course of the four
 899 experiments for the three treatments: ambient, medium, and high, nominally targeting pCO₂ levels of 400,
 900 800, and 1200 μatm, respectively. Water changes happened at weekly intervals, at which time dissolved
 901 inorganic carbon (DIC) and total alkalinity (TA) were measured. The TA/DIC measurements of ingoing pre-
 902 bubbled water entering the carboys are labelled “In” and the TA/DIC measurements of outgoing water
 903 leaving the carboys are labelled “Out”. Mid-week measurements of pH were made between water changes,
 904 labelled “Mid.” “Out” and “Mid” measurements shown are an average of the 2-3 carboys for each treatment,
 905 while “In” is a single measurement from the pre-bubbled holding tanks for each treatment. For the ingoing
 906 and outgoing water, DIC/TA measurements were used to calculate the values in the last three columns: pH,
 907 dissolved CO₂ (pCO₂), and aragonite saturation state (Ω_A). Mid-week measurements of pH were used with
 908 the nearest measurement of TA in time to calculate the pCO₂ and Ω_A values to estimate the carbonate
 909 chemistry between water changes.

Cruise	Treat	Day	Water Change	MEASURED			CALCULATED		
				DIC (μmol/kg)	TA (μmol/kg)	pH	pH	pCO ₂ (μatm)	Ω _A
Apr '14	Ambient	0	In	2058	2216	---	8.03	390	1.76
		1	Mid	---	---	7.96	---	470	1.54
		3	Mid	---	---	7.97	---	450	1.57
		5	Mid	---	---	7.99	---	440	1.62
		7	Out	2093	2234	---	7.96	470	1.54
		7	In	2068	2216	---	8.01	420	1.68
		8	Mid	---	---	7.97	---	450	1.58
		10	Mid	---	---	7.96	---	460	1.54
		13	Mid	---	---	7.98	---	440	1.59
		14	Out	2082	2215	---	7.97	460	1.55
		26	Mid	---	---	8.03	---	390	1.77
	29	Mid	---	---	8.03	---	390	1.74	
	Medium	0	In	2092	2214	---	7.94	500	1.45
		1	Mid	---	---	7.75	---	790	0.99
		3	Mid	---	---	7.77	---	760	1.02
		5	Mid	---	---	7.78	---	750	1.05
		7	Out	2175	2227	---	7.72	860	0.93
		7	In	2147	2217	---	7.78	740	1.05
		8	Mid	---	---	7.72	---	860	0.92
		10	Mid	---	---	7.70	---	910	0.88
		13	Mid	---	---	7.73	---	830	0.95
		14	Out	2166	2222	---	7.73	830	0.95
		26	Mid	---	---	7.79	---	710	1.09
	29	Mid	---	---	7.80	---	710	1.09	
	High	0	In	2111	2215	---	7.88	570	1.31
		1	Mid	---	---	7.59	---	1180	0.69
		3	Mid	---	---	7.61	---	1110	0.73
		5	Mid	---	---	7.68	---	940	0.86
		7	Out	2210	2220	---	7.57	1230	0.67
		7	In	2184	2216	---	7.65	1010	0.80
		8	Mid	---	---	7.57	---	1240	0.67
		10	Mid	---	---	7.55	---	1280	0.65
		13	Mid	---	---	7.58	---	1220	0.68
14		Out	2202	2219	---	7.60	1150	0.72	
26		Mid	---	---	7.58	---	1200	0.69	
29	Mid	---	---	7.60	---	1150	0.72		
	Ambient	0	In	2016	2176	---	8.04	379	1.77

Aug '14		1	Mid	---	---	7.99	---	430	1.58		
		3	Mid	---	---	7.92	---	510	1.38		
		6	Mid	---	---	7.95	---	470	1.47		
		7	Out	2052	2182	---	7.96	460	1.50		
		7	In	2028	2183	---	8.03	390	1.73		
		8	Mid	---	---	7.99	---	430	1..60		
		11	Mid	---	---	7.99	---	430	1.60		
		14	Out	2039	2185	---	8.00	414	1.65		
		Medium	0	In	2103	2162	---	7.74	790	0.95	
			1	Mid	---	---	7.71	---	840	0.90	
			3	Mid	---	---	7.69	---	890	0.85	
			6	Mid	---	---	7.72	---	840	0.92	
			7	Out	2125	2194	---	7.78	750	1.04	
			7	In	2104	2180	---	7.80	690	1.07	
	8		Mid	---	---	7.70	---	870	0.89		
	11		Mid	---	---	7.69	---	900	0.84		
	High	14	Out	2085	2198	---	7.91	540	1.38		
		0	In	2082	2177	---	7.86	590	1.22		
		1	Mid	---	---	7.59	---	1150	0.69		
		3	Mid	---	---	7.55	---	1260	0.63		
		6	Mid	---	---	7.58	---	1190	0.67		
		7	Out	2160	2186	---	7.63	1060	0.75		
		7	In	2143	2186	---	7.69	910	0.85		
		8	Mid	---	---	7.60	---	1120	0.71		
		11	Mid	---	---	7.64	---	1030	0.77		
		14	Out	2150	2198	---	7.70	880	0.89		
		Nov '14	Ambient	0	In	2062	2197	---	7.98	440	1.57
				6	Mid	---	---	8.07	---	360	1.89
7				Out	2118	2233	---	7.93	520	1.42	
7				In	2066	2195	---	7.97	460	1.52	
8	Mid			---	---	8.01	---	410	1.65		
10	Mid			---	---	7.99	---	430	1.58		
14	Out			2065	2198	---	7.98	440	1.55		
Medium	0			In	2129	2197	---	7.78	730	1.03	
	6		Mid	---	---	7.79	---	730	1.06		
	7		Out	2234	2234	---	7.55	1320	0.64		
	7		In	2142	2194	---	7.73	830	0.92		
	8		Mid	---	---	7.73	---	830	0.92		
	10		Mid	---	---	7.72	---	840	0.92		
	14		Out	2154	2201	---	7.71	870	0.89		
	High		0	In	2153	2196	---	7.70	890	0.86	
6			Mid	---	---	7.63	---	1080	0.76		
7			Out	2241	2239	---	7.54	1350	0.62		
7			In	2185	2191	---	7.57	1230	0.65		
8			Mid	---	---	7.58	---	1200	0.67		
10			Mid	---	---	7.57	---	1240	0.64		
14			Out	2205	2206	---	7.55	1290	0.63		
Apr '15			Ambient	0	In	2081	2218	---	7.99	440	1.59
	7			Out	2082	2222	---	8.00	430	1.62	
	7			In	2077	2212	---	7.98	440	1.58	
	7			Mid	---	---	8.01	---	420	1.65	
	11			Mid	---	---	7.99	---	430	1.61	
	14			Out	2085	2222	---	7.99	440	1.60	

		14	In	2108	2257	---	8.01	420	1.72	
		16	Mid	---	---	8.02	---	410	1.73	
		18	Mid	---	---	8.01	---	420	1.70	
	Medium	0	In	2153	2229	---	7.81	700	1.10	
		7	Out	2166	2222	---	7.74	820	0.95	
		7	In	2147	2211	---	7.77	760	1.01	
		7	Mid	---	---	7.79	---	720	1.06	
		11	Mid	---	---	7.82	---	680	1.12	
		14	Out	2143	2225	---	7.83	660	1.15	
		14	In	2173	2253	---	7.82	680	1.14	
		16	Mid	---	---	7.79	---	740	1.06	
		18	Mid	---	---	7.78	---	750	1.05	
		High	0	In	2191	2223	---	7.66	1000	0.80
			7	Out	2208	2221	---	7.59	1170	0.70
	7		In	2208	2209	---	7.55	1300	0.62	
	7		Mid	---	---	7.64	---	1050	0.76	
	11		Mid	---	---	7.63	---	1070	0.75	
	14		Out	2201	2214	---	7.59	1190	0.70	
	14		In	2198	2251	---	7.73	850	0.94	
	16		Mid	---	---	7.59	---	1190	0.70	
18	Mid		---	---	7.59	---	1200	0.70		

910
911